



Published in final edited form as:

Invest Ophthalmol Vis Sci. 2007 November ; 48(11): 5023–5029.

Neutrophil Interactions with Keratocytes during Corneal Epithelial Wound Healing: A Role for CD18 Integrins

Matei S. Petrescu¹, Chonna L. Larry², Robert A. Bowden², George W. Williams³, Debjani Gagen⁴, Zhijie Li^{4,5}, C. Wayne Smith⁴, and Alan R. Burns^{4,6}

¹Department of Pediatrics, Critical Care Section, Baylor College of Medicine, Houston, Texas

²US Military Academy, West Point, New York

³Department of Anesthesiology, Case School of Medicine, Cleveland, Ohio

⁴Department of Pediatrics, Children's Nutrition Research Center, Baylor College of Medicine, Houston, Texas

⁵Institute of Tissue Transplantation and Immunology, Jinan University, Guangzhou, China

⁶Section of Cardiovascular Sciences, Department of Medicine, Baylor College of Medicine, Houston, Texas

Abstract

PURPOSE—To determine the role of keratocytes and leukocyte β_2 (CD18) integrins in neutrophil (PMN) migration through the corneal stroma after epithelial scrape injury.

METHODS—Using C57BL/6 wild-type and CD18^{-/-} mice, corneas were excised at 6 hours (wild-type) or 24 hours (CD18^{-/-}) after central corneal epithelial abrasion, time points determined previously to have similar levels of emigrated PMNs. Corneas were prepared for ultrastructural morphometric analysis of PMNs, keratocyte networks, and collagen.

RESULTS—Transmission electron microscopy revealed intact keratocyte networks within the paralimbus that were morphometrically similar, regardless of epithelial injury or mouse genotype. Secondary to epithelial abrasion, extravasated PMNs within the paralimbus developed close contacts with keratocytes and collagen. In wild-type mice, 40% of the PMN surface was in contact with the keratocyte surface, and this value decreased to 10% in CD18^{-/-} mice. PMN contact with collagen was similar in wild-type and CD18^{-/-} mice, with approximately 50% of the PMN surface contacting the collagen fibrils. Since corneal edema resulting from scrape injury was similar, regardless of genotype and did not involve structural changes in collagen fibrils, these data favor a direct role for CD18 in mediating PMN contact with keratocytes.

CONCLUSIONS—The data show that in response to epithelial scrape injury, PMN migration in the corneal stroma involves close contact between keratocytes and collagen. Although PMN-keratocyte contacts require CD18 integrins, contact with collagen is CD18 independent. Fundamentally, PMN migration along keratocyte networks constitutes the beginning of a new experimental concept for understanding leukocyte migration within the wounded cornea.

The high incidence of direct corneal injury and increased availability of corrective refractive surgery (e.g., LASIK, PRK), with its accompanying corneal complications, have made clear the need for a better understanding of the intimate events that occur during corneal wound

Corresponding author: Alan R. Burns, Section of Cardiovascular Sciences, Department of Medicine, Baylor College of Medicine, Room 515B, One Baylor Plaza, Houston, TX 77030; aburns@bcm.tmc.edu.

Disclosure: M.S. Petrescu, None; C.L. Larry, None; R.A. Bowden, None; G.W. Williams, None; D. Gagen, None; Z. Li, None; C.W. Smith, None; A.R. Burns, None

healing.¹ Recently, our laboratory reported that neutrophils (PMNs) enter the corneal stroma shortly after epithelial scrape injury, and their presence appears to facilitate wound closure.² PMN transendothelial migration requires the leukocyte β_2 integrin CD18. In injured corneas of CD18^{-/-} mice, both PMN extravasation and wound closure are delayed by 24 hours and 6 hours, respectively.²

Although the precise mechanisms underlying PMN migration in the corneal stroma are poorly understood, it has been suggested that PMN migration within extravascular tissue (i.e., interstitium) is facilitated by integrin-dependent adhesive contacts with the structural elements of the extracellular matrix (e.g., collagen).³ However, migrating PMNs also develop adhesive contacts with resident interstitial cells.⁴ In the corneal stroma, the primary interstitial cell is the keratocyte, and each keratocyte joins with a neighboring keratocyte to form a cellular network.⁵ Keratocyte networks lie between the orthogonally arranged collagen layers, extending from limbus to limbus. Our preliminary observations suggested that in response to epithelial scrape injury, migrating PMNs develop close surface contacts with keratocytes,⁶ raising the possibility that keratocyte networks provide a contact guidance mechanism for PMNs migrating into the injured cornea, functioning as a “cellular highway” during leukocyte trafficking.

The purpose of the present study was to use a mouse model of corneal epithelial abrasion to obtain quantitative data on PMN interactions with structural matrix elements (collagen) and resident interstitial cells (keratocytes) during wound healing. In addition, we wanted to examine the “extravascular” role of the leukocyte β_2 integrin (CD18) in PMN contacts with collagen and keratocytes. Our results document for the first time that migrating PMNs make extensive surface contacts with keratocytes and that this heterotypic cell interaction requires CD18 integrins.

METHODS

Animals

Ten C57BL/6 mice wild-type were purchased from Harlan (Indianapolis, IN). Ten CD18^{-/-} mice were backcrossed at least 10 generations with C57BL/6 mice. Mice used in this study were 6 to 12 weeks old, weighed 18 to 24 g, and were treated according to the ARVO Statement for the Use of Animals in Ophthalmic and Vision Research and institutional and federal guidelines.

Wound Model

Mice were anesthetized by intraperitoneal injection of pentobarbital sodium solution (50 mg/kg; Nembutal; Ovation Pharmaceuticals, Deerfield, IL). The central corneal epithelium was demarcated with a 2-mm trephine and then removed using a diamond blade (Accutome, Malvern, PA) for refractive surgery under a dissecting microscope. This method does not injure the epithelial basal lamina or underlying stroma.² Buprenorphine (0.1 mg/kg) was administered to all animals to relieve pain after surgery. Adequacy of anesthesia was assessed by lack of withdrawal reflex to a toe pinch and was maintained by supplemental doses of pentobarbital. Wounded corneas were dissected from humanely killed (CO₂ inhalation followed by cervical dislocation) mice 6 and 24 hours after injury in wild-type and CD18^{-/-} mice, respectively. These time points were chosen because they have equivalent levels of PMN extravasation, as determined in our previous study.² Briefly, the removal of a 2-mm diameter area of epithelium from the center of the cornea of wild-type mice results in PMN extravasation from the limbal vessels. PMN migration into the cornea begins around 6 hours, and peak PMN migration into the central avascular cornea occurs 12 to 18 hours after injury. In contrast, PMN extravasation in the corneas of CD18^{-/-} mice is delayed until 24 hours after injury, and PMN migration into

the central cornea does not peak until 30 hours. These results are in keeping with the known “intravascular” role that CD18 plays in regulating PMN migration across the endothelium.

Electron Microscopy

Corneas were excised and fixed in buffer (0.1 M sodium cacodylate, pH 7.2) containing 2.5% glutaraldehyde for 2 hours at room temperature. Each cornea was sliced vertically into four quadrants and postfixed in 1% tannic acid for 5 minutes, followed by postfixation with 1% osmium tetroxide. All samples were dehydrated in a graded ethanol series and finally embedded in Araldite resin. Thin (80- to 100-nm) sections were cut with an ultramicrotome (RMC 7000; Boeckeler Instruments, Inc., Tucson, AZ) and were stained with uranyl acetate and lead citrate before viewing on a transmission electron microscope (200 CX; JEOL, Tokyo, Japan).

For morphometric analysis, all electron micrographs were recorded from the paralimbal region, defined as the portion of nonvascular corneal stroma immediately adjacent and central to the vascular limbus.

Electron micrographs were collected from anterior (upper one third) and posterior (lower one third) aspects of the paralimbal stroma. PMNs (5000–7300× magnification; 10 profiles per cornea), keratocytes (3700× magnification; 10 nonoverlapping micrographs per cornea), and collagen fibrils (37000× magnification; 100 cross-sectional views of collagen bundles per cornea) were photographed randomly by scanning the cornea in a systematic rasterized pattern, thus eliminating observer bias and satisfying the morphometric criteria for systematic uniform random sampling.⁷

Corneal Thickness Measurements

Corneas were prepared for electron microscopy (see above). Thick (0.5 μm) sections were cut from the corneas, stained with 1% toluidine blue O, and examined by light microscopy at 40× magnification. The paralimbus was identified, and three stromal measurements, spaced laterally at 50-μm intervals perpendicular to the Descemet membrane, were made, and the mean was calculated and reported as corneal stromal thickness at the paralimbus. The paralimbus was defined as a circumferential zone, 0.53 mm in width (i.e., one 40× microscope field), located immediately central to the limbus.⁸ By multiplying the surface area of the paralimbal zone (μm²) by the thickness of each corneal stroma (μm), we were able to calculate the volume of the paralimbal stroma.

Morphometric Analysis

All photomicrographs were digitized by scanning of negatives at high resolution (16 bit grayscale, 600 line/inch; ScanMaker 8700 [Microtek USA, Carson, CA]). An image editing system (Photoshop; Adobe Systems Inc., San Jose, CA) was used for image analysis.

Stereology is the science involved in making accurate three-dimensional (3D) morphometric estimations based on 2D measurements. In this study, a manual point/intercept counting method was used for the analysis of PMNs and keratocytes. The technique involves casting a cycloid grid over the micrograph and counting the number of intersections between the grid points/lines and the cell profile (Fig. 1). Because the cornea is not isotropic and has a preferred, nonrandom (layered) orientation of cells and collagen, the cycloid grid removes the inherent bias that is built into the cornea. The grid is composed of sinusoidal lines and associated target points with a known ratio of length of line per point. For every analyzed image, the grid was randomly cast in the X-Y plane, carefully maintaining the direction of the grid perpendicular to the layering of the collagen.

Using the cycloid grid approach, PMN surface density (S_v , μm^{-1}) was calculated using an established stereology formula:

$$S_v = \frac{2 \cdot \sum_{i=1}^n I_i}{l/p \cdot \sum_{i=1}^n P_i}$$

where l/p is the length of test line per grid point (corrected for magnification), I is the number of intersections between the grid and the PMN membrane, and P is the number of grid points lying over the PMN (cytoplasm and nucleus). The amount of PMN surface (i.e., percentage of S_v) in close contact with collagen fibrils or keratocytes was calculated. Close contact was defined as 25 nm or less, the distance over which cell adhesion molecules might be expected to mediate cell adhesion.⁹ For paralimbal keratocytes, membrane surface area (μm^2) was calculated by multiplying keratocyte surface density (keratocyte surface relative to corneal stromal volume) by the volume of the paralimbal stroma. To assess the shape¹⁰ of the keratocyte network, the amount of keratocyte surface relative to keratocyte volume was calculated using the formula for S_v above.

Collagen fibril measurements for diameter and spacing were made from cross-sectional views of collagen bundles. Collagen bundles were defined as a central collagen fibril with five or six surrounding fibrils forming a pentagon or a hexagon.^{11,12} For each bundle, the fibril diameters were measured and the center–center distance between the central fibril and each outer fibril (i.e., the interfibril spacing) was determined (Fig. 2). A carbon diffraction line grating replica with a known line density (1250 lines/mm) was photographed at 37,000 \times magnification and was used as an internal reference scale when making collagen measurements.

Statistical Analysis

Data analysis was performed using one-way repeated-measures ANOVA, followed by a Newman-Keuls posttest. $P < 0.05$ was considered significant. Data are expressed as mean \pm SEM.

RESULTS

In the present study, we wanted to examine the “extravascular” role of CD18 in mediating PMN migration within the corneal stroma. Because the kinetics of PMN emigration in CD18^{-/-} mice lags behind that of wild-type mice, we examined injured corneas in wild-type and CD18^{-/-} mice when PMN extravasation levels were similar. For this reason, wild-type and CD18^{-/-} mouse corneas were studied at 6 hours and 24 hours after injury, respectively, time points previously established as having comparable levels of PMN extravasation.²

After corneal epithelial abrasion, major changes occur in the stroma underneath the injury, notably corneal edema and keratocyte death. Specifically, keratocyte loss occurs in the central cornea (Fig. 3) as the result of apoptosis.¹³ Migrating PMNs within the central cornea are limited to surface contacts with the collagen matrix alone. In this study, our analysis of PMN stromal migration was focused on the paralimbus, an area 1 mm from the initial epithelial wound edge, where the epithelium is not directly injured and keratocytes remain viable (Fig. 4). As expected, after central epithelial abrasion, PMN migration into the paralimbus was evident in corneas of wild-type and CD18^{-/-} mice 6 and 24 hours after injury, respectively. Looking at the disposition of PMNs in relation to a virtual line dividing the corneal stroma into anterior and posterior halves, we found that PMNs migrate preferentially in the anterior half of the stroma (Fig. 5) in wild-type (90% \pm 4%) and CD18^{-/-} (75% \pm 13%) mice ($P < 0.05$). At an ultrastructural level, PMNs appeared to make close surface contact with resident

interstitial cells (keratocytes) and with the extracellular matrix (collagen fibrils; Fig. 6). To determine the relative amount of PMN surface in close contact with keratocytes and collagen, we undertook an ultrastructural morphometric analysis of injured corneas.

Table 1 shows that in wild-type mice, approximately half the PMN surface was in close contact with keratocytes and that the other half was in close contact with collagen. By comparison, in CD18^{-/-} mice, PMN close surface contact with keratocytes was reduced by 75% ($P < 0.05$) whereas contact with collagen was unaffected (Table 1; Fig. 6). Although these data suggest CD18 mediates PMN surface interactions with keratocytes, other explanations are possible. For example, less keratocyte surface available for contact in injured corneas of CD18^{-/-} mice could have accounted for the diminished interactions with PMNs. In addition, after epithelial injury, the corneal stroma became edematous. Although the number of PMNs entering the paralimbus was similar in wild-type and CD18^{-/-} mouse corneas 6 and 24 hours after injury, respectively, the degree of tissue edema might have been different, and this difference could have favored diminished PMN contact with keratocytes in CD18^{-/-} mouse corneas. Indeed, Table 1 shows that approximately 94% of the wild-type PMN surface was in close contact with keratocytes or collagen. By comparison, in CD18^{-/-} mice, only approximately 62% of the PMN surface was engaged with keratocytes or collagen; the remaining “free” surface (approximately 38%) was adjacent to electron translucent “space” created by edema (Fig. 6). For these reasons, we undertook three additional ultrastructural morphometric analyses to clarify the role for CD18 in mediating PMN contact with keratocytes.

The first morphometric index calculated was the total amount of keratocyte surface area within the paralimbal stroma that was available for contact with PMNs. This is an important consideration because PMN interaction with keratocytes ultimately depends on the amount of keratocyte surface available for contact. This value is not just dependent on keratocyte density (i.e., number of keratocytes per unit volume of corneal stroma), it also depends on the size (volume) of the individual keratocytes. Our morphometric analysis revealed no statistically significant difference in keratocyte surface area between wild-type and CD18^{-/-} corneas, regardless of the presence of injury or location within the stroma (anterior or posterior; Table 2). Even though there appears to be a 30% decline in anterior keratocyte surface area in CD18^{-/-} mice after injury, possibly accounting for some of the reduction in CD18^{-/-} PMN contact with keratocytes, the decline did not reach statistical significance ($P = 0.23$). The second morphometric index calculated was the amount of keratocyte surface relative to its own keratocyte volume, an indicator of cell shape. For example, if the keratocytes became contracted or swollen as a result of injury, their surface-to-volume ratio would change. However, our data show that the keratocyte surface-to-volume ratio was not significantly different in wild-type and CD18^{-/-} mice in injured or uninjured corneas, regardless of location (anterior or posterior cornea; Fig. 7). Hence, not only is the amount of surface membrane available for contact with PMNs comparable and unaffected by corneal injury, the shape of the paralimbal keratocyte network remains similar in wild-type and CD18^{-/-} mouse corneas. The first two analyses suggest the paralimbal keratocyte network is unaffected by injury or CD18 genotype.

After epithelial injury, the paralimbal stroma was clearly edematous, as evidenced by an increase in stromal thickness. The data show that the increase in thickness was similar in wild-type and CD18^{-/-} mice (1.2 ± 0.1 -fold vs. 1.15 ± 0.1 -fold, respectively). To understand better how edema affects the organization of the paralimbal stroma, we undertook a third morphometric study to determine whether edema altered collagen fibril diameter and spacing. The data show that collagen fibril diameters, in the anterior and posterior paralimbal stroma, were similar in wild-type and CD18^{-/-} mice and were not affected by epithelial abrasion (Table 3). Similarly, collagen fibril spacing was not significantly different between wild-type and CD18^{-/-} corneas, regardless of injury or location (anterior or posterior stroma) (Fig. 8). Hence,

in our injury model, stromal thickening (edema) that accompanies corneal epithelial abrasion does not involve structural changes in collagen fibrils.

DISCUSSION

The purpose of this study was to evaluate PMN interactions with keratocytes and collagen during corneal wound healing after epithelial abrasion and to determine whether these extravascular interactions are mediated by CD18. The results of this study support the conclusion that in response to epithelial abrasion, PMNs migrate preferentially in the anterior corneal stroma and make surface contact with keratocytes and collagen as they journey through the paralimbus. Contact with keratocytes, but not collagen, is mediated by CD18 adhesion molecules. Diminished PMN contact with keratocytes in the absence of CD18 does not appear to result from decreased keratocyte surface availability. In the current study, the data supporting these conclusions are as follows: (1) most PMNs that migrate in the paralimbus are located in the anterior stroma; (2) in wild-type mice, half the migrating PMN surface is in contact with keratocytes and the other half is in contact with collagen, and though CD18^{-/-} PMNs establish similar amounts of surface contact with collagen as wild-type PMNs, they show a significant decrease in contact with keratocytes; (3) the shape and extent of the keratocyte network in the paralimbus is similar in wild-type and CD18^{-/-} mice.

To our knowledge this is the first study to quantify the complex interaction between PMNs and the keratocyte network after epithelial injury, and it lends further support to the concept that the “keratocyte highway” regulates leukocyte trafficking.⁶ Interestingly, interactions between emigrated PMNs and interstitial resident cells have also been reported in other systems. Behzad et al.,¹⁴ using a streptococcal pneumonia model in rabbits, observed close contact between PMNs and lung fibroblasts. In vitro, canine PMNs have been shown not only to adhere to lung fibroblasts but also to engage in CD18-dependent motility after activation with PAF and IL-8.¹⁵ Similar reports exist for human PMN migration on fibroblasts from synovia, lung, and skin, in which migration was found to be dependent on β_1 and β_2 integrins.^{16–18}

Therefore, do keratocytes express CD18 ligands? Intracellular adhesion molecule-1 (ICAM-1), a well-recognized ligand for CD18-dependent PMN adhesion,¹⁹ is expressed on cultured corneal fibroblasts.²⁰ ICAM-1 supports the binding of CD11a/CD18 and CD11b/CD18.¹⁹ More recently, junctional adhesion molecule-C (JAM-C) was also shown to be expressed on cultured human corneal fibroblasts.²¹ JAM-C is known to mediate CD11b/CD18-dependent PMN adhesion to epithelia,²² endothelia,²³ and platelets.²⁴ Whether corneal keratocytes express ICAM-1 and JAM-C in vivo, before and after epithelial abrasion, remains to be determined.

Preferential PMN migration within the anterior aspect of the corneal stroma has been reported in other models of corneal injury. After intrastromal injection of LPS, Carlson et al.²⁵ found predominant anterior migration of PMNs in the center of the cornea. One explanation for preferential PMN anterior migration would be anterior–posterior differences in the keratocyte network or the collagen matrix. Indeed, differences between anterior and posterior keratocyte densities in other species have been proposed. For example, in humans and rabbits, keratocyte nuclear density appears to decrease gradually from anterior and posterior.^{26–28} These studies are based on confocal microscopy images and counts of cell nuclei. The distribution of keratocytes is less clear in rodents because keratocyte nuclei are less reflective, precluding confocal microscopy density measurements.²⁶ In our study, we did not count nuclei. Instead, we used a morphometric approach to assess keratocyte membrane surface area in the anterior and posterior stroma. The results suggest that in C57B1/6 mice, the keratocyte surface is similar in the anterior and posterior aspects of the paralimbal stroma. If the mouse keratocyte

distribution is similar to that of humans and rabbits (i.e., lower cell density in the posterior stroma), the posterior keratocytes would have to be larger than the anterior keratocytes. Indeed, in a study of porcine corneas, Hahnel et al.²⁹ found increased cell volumes and surface areas in posterior keratocytes, despite a decrease in cell density compared to anterior keratocytes. Regardless, our data argue against anterior/posterior keratocyte network differences as an explanation for preferential anterior PMN migration in the injured mouse cornea.

With respect to potential anterior/posterior differences in the collagen matrix, our data clearly show that collagen fibril diameter and spacing were similar, regardless of location (anterior or posterior), and unchanged by corneal injury or genotype. Moreover, our findings are similar to published mouse corneal data obtained by electron microscopy³⁰ or x-ray diffraction.³¹ The observation that stromal thickness increased approximately 20% after corneal injury in wild-type and CD18^{-/-} mice leads us to conclude that in our injury model, edema must be largely confined to the tissue space between the collagen layers, where the keratocyte networks are located. Support for this conclusion can be found in an ex vivo rat skin model of hydration, where tissue edema occurs at the interface between collagen and fibroblasts, without affecting collagen spacing or fibroblast volume.³² In the cornea, the formation of stromal edema between collagen layers, where PMNs migrate after epithelial abrasion, likely facilitates PMN locomotion by opening migration passageways.

In conclusion, our data show that in response to epithelial scrape injury, PMN migration in the corneal stroma involves close contact with keratocytes and collagen. Although PMN–keratocyte contact requires CD18 integrins, contact with collagen is CD18 independent. Fundamentally, PMN migration along keratocyte networks constitutes the beginning of a new experimental concept for understanding leukocyte migration with the wounded cornea.

Acknowledgments

The authors thank Evelyn Brown for providing excellent technical support.

Supported by National Heart, Lung, and Blood Institute Grant HL070357, National Institute of Allergy and Infectious Diseases Grant AI46773, and National Natural Science Foundation of China Grant 39970250. The views expressed in the article are those of the authors and do not reflect the official policy of the Department of the Army, the Department of Defense or the U.S. Government.

References

1. Netto MV, Mohan RR, Ambrosio R Jr, Hutcheon AE, Zieske JD, Wilson SE. Wound healing in the cornea: a review of refractive surgery complications and new prospects for therapy. *Cornea* 2005;24:509–522. [PubMed: 15968154]
2. Li Z, Burns AR, Smith CW. Two waves of neutrophil emigration in response to corneal epithelial abrasion: distinct adhesion molecule requirements. *Invest Ophthalmol Vis Sci* 2006;47:1947–1955. [PubMed: 16639002]
3. Lindbom L, Werr J. Integrin-dependent neutrophil migration in extravascular tissue. *Semin Immunol* 2002;14:115–121. [PubMed: 11978083]
4. Burns AR, Smith CW, Walker DC. Unique structural features that influence neutrophil emigration into the lung. *Physiol Rev* 2003;83:309–336. [PubMed: 12663861]
5. Poole CA, Brookes NH, Clover GM. Confocal imaging of the human keratocyte network using the vital dye 5-chloromethylfluorescein diacetate. *Clin Exp Ophthalmol* 2003;31:147–154.
6. Burns AR, Li Z, Smith CW. Neutrophil migration in the wounded cornea: the role of the keratocyte. *Ocul Surface* 2005;3:S173–S176.
7. Howard, CV.; Reed, MG. *Unbiased Stereology—Three-Dimensional Measurement in Microscopy*. 1st ed. New York: Springer-Verlag; 1998.

8. Li Z, Rumbaut RE, Burns AR, Smith CW. Platelet response to corneal abrasion is necessary for acute inflammation and efficient re-epithelialization. *Invest Ophthalmol Vis Sci* 2006;47:4794–4802. [PubMed: 17065490]
9. Springer TA. Adhesion receptors of the immune system. *Nature* 1990;346:425–434. [PubMed: 1974032]
10. Weibel, ER. *Stereological Methods*. Vol. 1. London, UK: Academic Press; 1979. p. 204–210.p. 306
11. Kuwaba K, Kobayashi M, Nomura Y, Irie S, Koyama Y. Elongated dermatan sulphate in post-inflammatory healing skin distributes among collagen fibrils separated by enlarged interfibrillar gaps. *Biochem J* 2001;358:157–163. [PubMed: 11485563]
12. Muller LJ, Pels E, Schurmans LR, Vrensen GF. A new three-dimensional model of the organization of proteoglycans and collagen fibrils in the human corneal stroma. *Exp Eye Res* 2004;78:493–501. [PubMed: 15106928]
13. Wilson SE. Role of apoptosis in wound healing in the cornea. *Cornea* 2000;19:S7–S12. [PubMed: 10832715]
14. Behzad AR, Chu F, Walker DC. Fibroblasts are in a position to provide directional information to migrating neutrophils during pneumonia in rabbit lungs. *Microvasc Res* 1996;51:303–316. [PubMed: 8992230]
15. Burns AR, Simon SI, Kukielka GL, et al. Chemotactic factors stimulate CD18-dependent canine neutrophil adherence and motility on lung fibroblasts. *J Immunol* 1996;156:3389–3401. [PubMed: 8617965]
16. Gao JX, Wilkins J, Issekutz AC. Migration of human polymorphonuclear leukocytes through a synovial fibroblast barrier is mediated by both beta 2 (CD11/CD18) integrins and the beta 1 (CD29) integrins VLA-5 and VLA-6. *Cell Immunol* 1995;163:178–186. [PubMed: 7541723]
17. Gao JX, Issekutz AC. Polymorphonuclear leucocyte migration through human dermal fibroblast monolayers is dependent on both beta 2-integrin (CD11/CD18) and beta 1-integrin (CD29) mechanisms. *Immunology* 1995;85:485–494. [PubMed: 7558139]
18. Shang XZ, Issekutz AC. Beta 2 (CD18) and beta 1 (CD29) integrin mechanisms in migration of human polymorphonuclear leucocytes and monocytes through lung fibroblast barriers: shared and distinct mechanisms. *Immunology* 1997;92:527–535. [PubMed: 9497495]
19. Burns, AR.; Rumbaut, RE. Mechanisms of neutrophil migration. In: Gabrilovich, DI., editor. *The Neutrophils: New Outlook for Old Cells*. London, UK: Imperial College Press; 2005. p. 110–114.
20. Kumagai N, Fukuda K, Fujitsu Y, Lu Y, Chikamoto N, Nishida T. Lipopolysaccharide-induced expression of intercellular adhesion molecule-1 and chemokines in cultured human corneal fibroblasts. *Invest Ophthalmol Vis Sci* 2005;46:114–120. [PubMed: 15623762]
21. Morris AP, Tawil A, Berkova Z, Wible L, Smith CW, Cunningham SA. Junctional adhesion molecules (JAMs) are differentially expressed in fibroblasts and co-localize with ZO-1 to adherens-like junctions. *Cell Commun Adhes* 2006;13:233–247. [PubMed: 16916751]
22. Zen K, Babbin BA, Liu Y, Whelan JB, Nusrat A, Parkos CA. JAM-C is a component of desmosomes and a ligand for CD11b/CD18-mediated neutrophil transepithelial migration. *Mol Biol Cell* 2004;15:3926–3937. [PubMed: 15194813]
23. Chavakis T, Keiper T, Matz-Westphal R, et al. The junctional adhesion molecule-C promotes neutrophil transendothelial migration in vitro and in vivo. *J Biol Chem* 2004;279:55602–55608. [PubMed: 15485832]
24. Santoso S, Sachs UJ, Kroll H, et al. The junctional adhesion molecule 3 (JAM-3) on human platelets is a counterreceptor for the leukocyte integrin Mac-1. *J Exp Med* 2002;196:679–691. [PubMed: 12208882]
25. Carlson EC, Drazba J, Yang X, Perez VL. Visualization and characterization of inflammatory cell recruitment and migration through the corneal stroma in endotoxin-induced keratitis. *Invest Ophthalmol Vis Sci* 2006;47:241–248. [PubMed: 16384969]
26. Labbe A, Liang H, Martin C, Brignole-Baudouin F, Warnet JM, Baudouin C. Comparative anatomy of laboratory animal corneas with a new-generation high-resolution in vivo confocal microscope. *Curr Eye Res* 2006;31:501–509. [PubMed: 16769609]

27. Patel S, McLaren J, Hodge D, Bourne W. Normal human keratocyte density and corneal thickness measurement by using confocal microscopy in vivo. *Invest Ophthalmol Vis Sci* 2001;42:333–339. [PubMed: 11157863]
28. Patel SV, McLaren JW, Camp JJ, Nelson LR, Bourne WM. Automated quantification of keratocyte density by using confocal microscopy in vivo. *Invest Ophthalmol Vis Sci* 1999;40:320–326. [PubMed: 9950589]
29. Hahnel C, Somodi S, Slowik C, Weiss DG, Guthoff RF. Fluorescence microscopy and three-dimensional imaging of the porcine corneal keratocyte network. *Graefes Arch Clin Exp Ophthalmol* 1997;235:773–779.
30. Chakravarti S, Petroll WM, Hassell JR, et al. Corneal opacity in lumican-null mice: defects in collagen fibril structure and packing in the posterior stroma. *Invest Ophthalmol Vis Sci* 2000;41:3365–3373. [PubMed: 11006226]
31. Quantock AJ, Meek KM, Chakravarti S. An x-ray diffraction investigation of corneal structure in lumican-deficient mice. *Invest Ophthalmol Vis Sci* 2001;42:1750–1756. [PubMed: 11431438]
32. Martel H, Walker DC, Reed RK, Bert JL. Dermal fibroblast morphology is affected by stretching and not by C48/80. *Connect Tissue Res* 2001;42:235–244. [PubMed: 11913768]

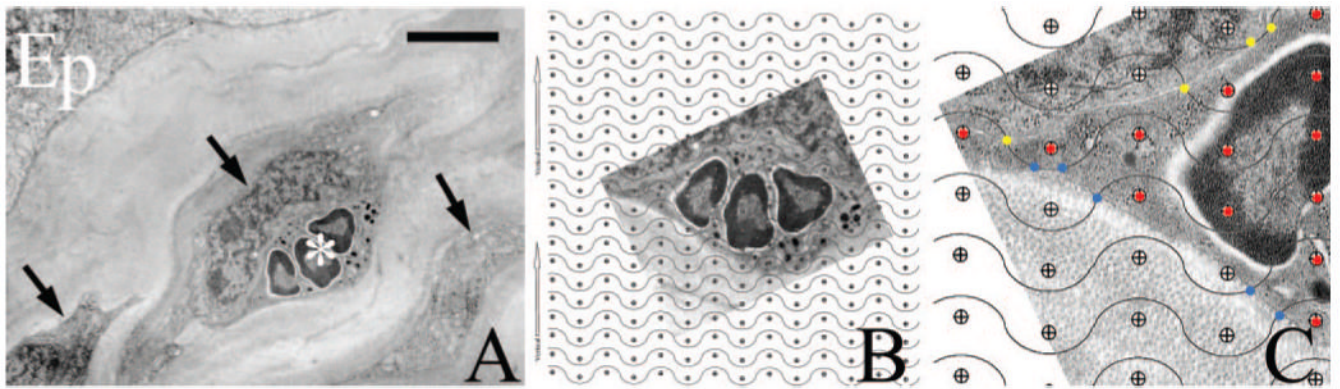


FIGURE 1.

Transmission electron micrographs of wild-type paralimbal stroma 6 hours after injury, illustrating the method used for morphometric analysis of PMN (*white asterisk*) contacts with keratocytes and collagen. The initial image (**A**) is rotated (**B**) to match the cycloid grid orientation. (**C**) Enlarged view of (**B**). The grid points and lines intersecting PMN contacts are colored according to the nature of the contact. Ep, corneal epithelium. *Black arrows*: keratocytes. *Red dots*: PMN body. *Yellow dots*: PMN close contact with keratocyte. *Blue dots*: PMN close contact with collagen. Scale bar, 2 μm .

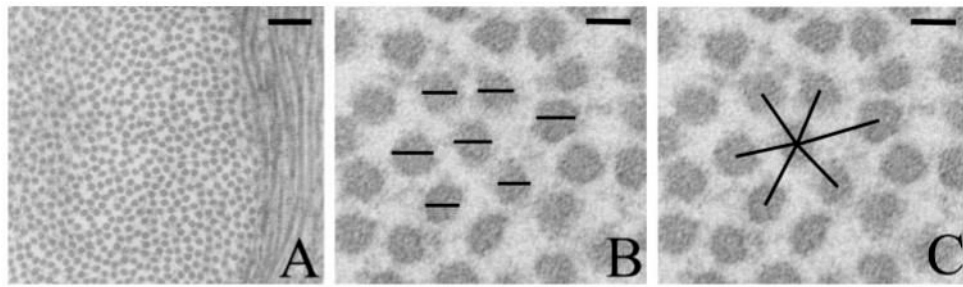


FIGURE 2.

Transmission electron micrographs of collagen fibrils in the paralimbal stroma of a wild-type cornea 6 hours after injury. For morphometric analysis, collagen fibrils were photographed in cross-section (**A**). Higher magnification (**B**, **C**) reveals collagen fibrils arranged in a hexagon around a central fibril. Collagen fibril diameters (**B**) and the distances between the central and outer fibrils (**C**) were measured. Scale bars: 200 nm (**A**), 30 nm (**B**, **C**).

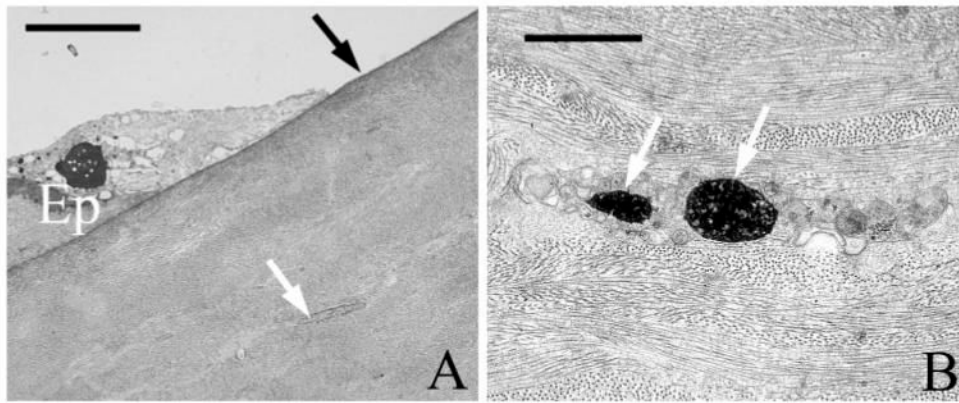


FIGURE 3. Transmission electron micrographs of wild-type cornea, 6 hours after injury. In the central abraded region (**A**), the Bowman membrane remains intact (*black arrow*), whereas injured keratocytes (*white arrow*) are present beneath the wound. Apoptotic bodies (*white arrows*, **B**) are frequently detected within injured keratocytes. Ep, corneal epithelium. Scale bars: 5 μm (**A**), 2 μm (**B**).

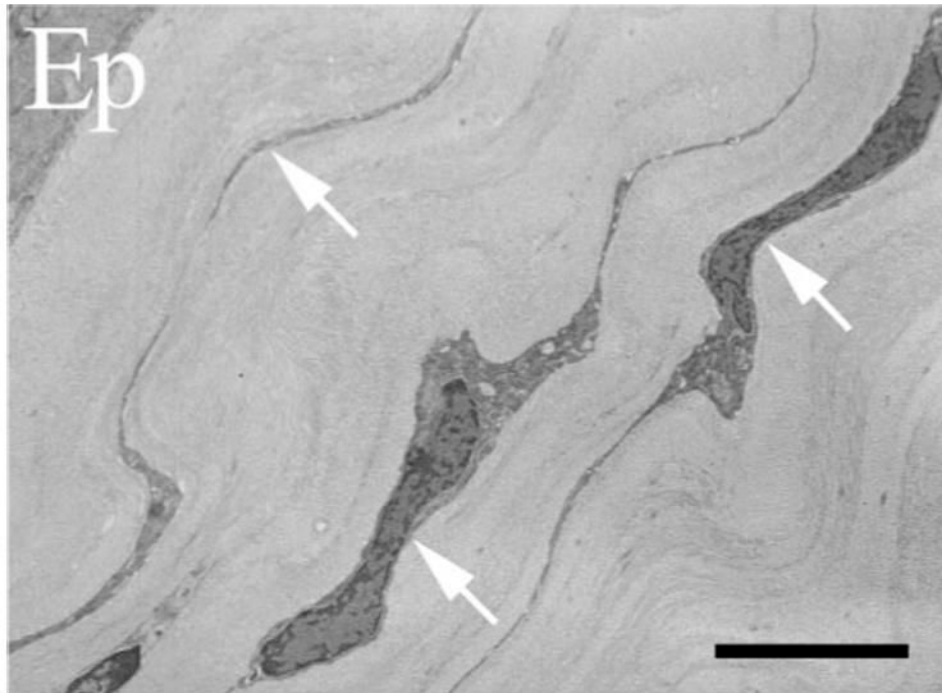


FIGURE 4. Transmission electron micrograph of CD18^{-/-} cornea 24 hours after injury. Keratocyte networks (*arrows*) remain intact under uninjured epithelium (Ep) overlying paralingual stroma. Scale bar, 5 μ m.

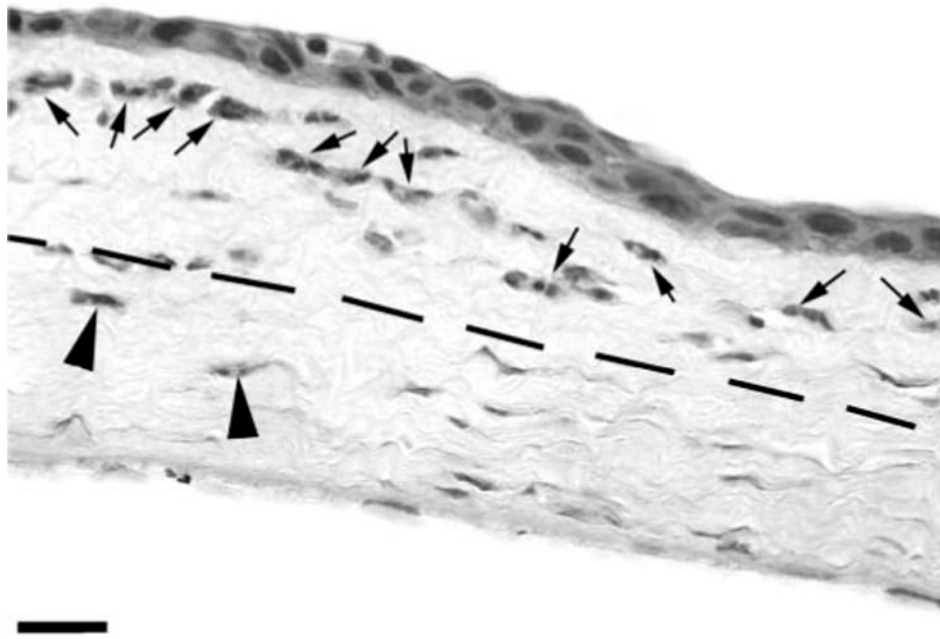


FIGURE 5. Light micrograph of wild-type cornea in cross-section, 6 hours after injury. PMNs migrate preferentially in the anterior half of the paralimbal corneal stroma (*arrows*, anterior PMNs; *arrowheads*, posterior PMNs). *Dashed line* divides corneal stroma into anterior and posterior halves. Scale bar, 15 μm .

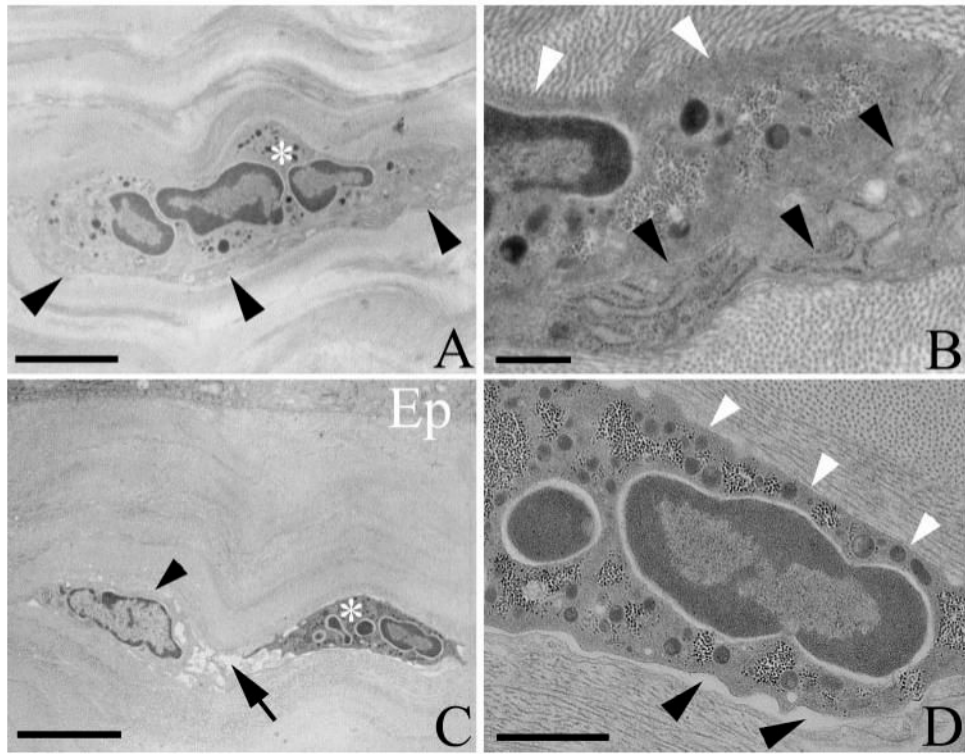


FIGURE 6.

Transmission electron micrographs of injured corneas in wild-type (**A, B**) and $CD18^{-/-}$ (**C, D**) mice. (**A**) Wild-type PMN (*white asterisk*) in close association with a keratocyte (*black arrowheads*). (**B**) Enlarged view of (**A**) shows that the PMN makes extensive close contact with collagen (*white arrowheads*) and the keratocyte (*black arrowheads*). (**C**) Migrating $CD18^{-/-}$ PMN (*white asterisk*) within the stroma beneath the paralimbal epithelium (Ep). A nearby keratocyte (*black arrowhead*) is surrounded by electron translucent space (edema; *black arrow*). (**D**) Enlarged view of (**C**). Note how the PMN establishes close contact with collagen (*white arrowheads*), whereas close contacts with the keratocyte are less evident, and the distance between opposing PMN and keratocyte surfaces is typically more than 25 nm (*black arrowheads*). Scale bars: 2 μm (**A**), 0.5 μm (**B**), 5 μm (**C**), 1 μm (**D**).

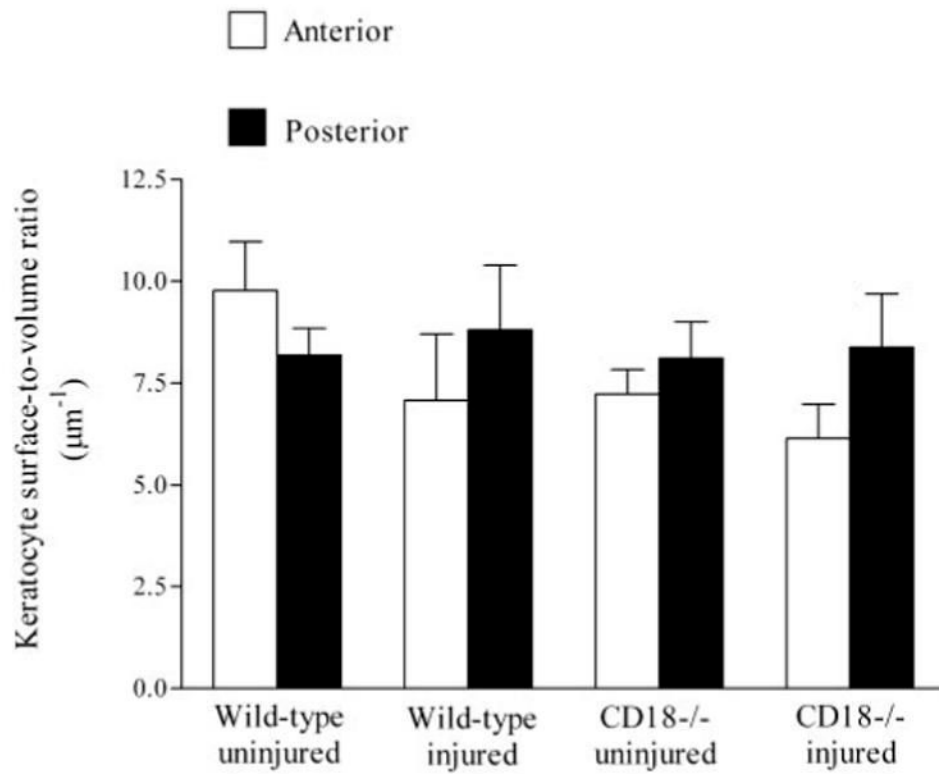


FIGURE 7. Paralimbal keratocyte surface–volume ratios within the anterior and posterior corneal stroma. Data expressed as mean \pm SEM.

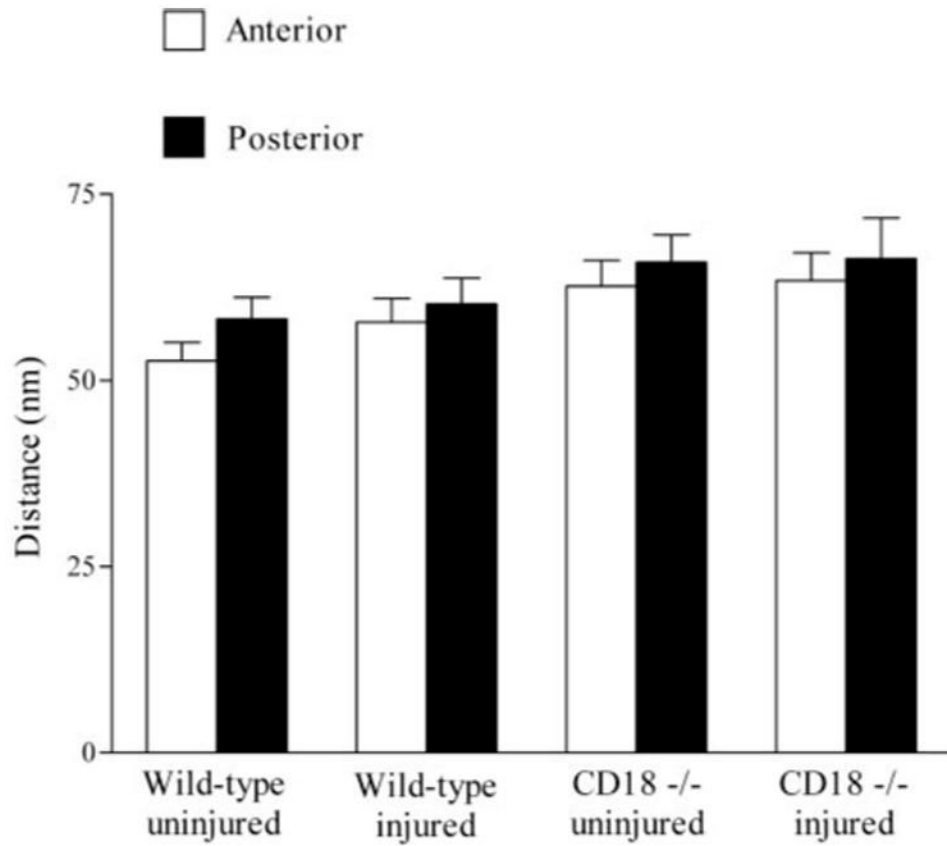


FIGURE 8. Collagen fibril spacing (distance) in anterior and posterior aspects of corneal stroma. Data expressed as mean \pm SEM.

TABLE 1

Percentage of PMN Surface in Close Contact (≤ 25 nm) with Keratocytes or Collagen Fibrils in the Paralimbus of Injured Corneas

Genotype	Contact with Keratocytes (%)	Contact with Collagen (%)
Wild-type	41.2 \pm 4.4	52.5 \pm 5.1
CD18 ^{-/-}	10.6 \pm 3.3*	51.0 \pm 5.5

Data are presented as mean \pm SEM. $n = 5$ for each genotype.

* $P < 0.05$ compared with wild-type.

TABLE 2Total Keratocyte Surface Area ($\times 10^6 \mu\text{m}^2$) within the Anterior and Posterior Aspects of the Paralimbal Stroma

Genotype	Uninjured		Injured	
	Anterior	Posterior	Anterior	Posterior
Wild-type	91.8 \pm 7.5	115.4 \pm 12.2	111.6 \pm 11.5	131.8 \pm 27.9
CD18 ^{-/-}	106.4 \pm 11.9	106.2 \pm 13.4	80.2 \pm 18.2	137.2 \pm 15.8

Data are presented as mean \pm SEM. $n = 5$ for each genotype.

TABLE 3

Paralimbal Collagen Fibril Diameter (nm)

Genotype	Uninjured		Injured	
	Anterior	Posterior	Anterior	Posterior
Wild-type	29 ± 1.4	33 ± 1.7	32 ± 1.2	36 ± 2.6
CD18 ^{-/-}	33 ± 2.8	36 ± 2.3	31 ± 1.9	36 ± 3.6

Data are presented as mean ± SEM. *n* = 5 for each genotype.